ORIGINAL PAPER

Geoelectric and mineralogical studies for foundation soil characterization in new Luxor city, Upper Egypt

Sayed Omer Elkhateeb[1] · Wael Dosoky[1] · Abdelnasser Mohamed[2] · Mahmoud A. Abbas[1]

Abstract

The new Luxor city was proposed by the Egyptian government as a new constructional and building site in order to face the increasing population density around the two banks of the river Nile. It is important prior construction of buildings to characterize the foundation soil. So, vertical electrical resistivity survey and mineralogical investigation were conducted for this purpose. The results obtained from the interpretation of the sounding data indicate that the lithological succession of the study area consists of four geoelectric layers. The top layer corresponds to the surface loose sediments of conglomerate, gravel, and sand. The second geoelectric layer is composed of sand and gravel. The third layer is composed of silty clay, sandy clay, and clayey sand. The fourth geoelectric layer is composed of dry sandstone. The X-ray diffraction (XRD) results of samples collected from the clay-rich layer revealed the presence of smectite mineral as predominate clay minerals which is characterized by its swell potentiality on wetting. Accordingly, the clay zone recorded within the third layer must be taken into consideration during designing the foundations at new Luxor city especially this layer was located at shallow depth range between 1.6 and 7.5 m and attains a relatively big thickness that reach up to 33.5 m in some parts. This study emphasizes the importance of the integration of geophysical investigation and mineralogical analysis of the foundation soil for optimal characterization of a site.

Keywords Geoelectric · Site characterization · New Luxor city · XRD · Smectite

Introduction

The construction of new cities and urban areas in desert lands is one of the sustainable development goals in Egypt in order to face the ever-increased population. Accordingly, the new Luxor city was chosen by the Egyptian government as a new constructional and building site to be one of the urban communities in Luxor district, Upper Egypt.

For a successful construction process for any engineering facility, sufficient information about the subsurface soil condition must not be neglected (Cosenza et al. 2006). These information can be obtained by utilizing geophysical methods which are faster and cheaper than conventionally

drilling and trenching operations (Legget and Karrow 1983; Okwueze et al. 1989; Gupta et al. 2019).

The application of geophysical methods has been increased and become a promising approach because they are quick, inexpensive, and non-destructive (Samouëlian et al. 2005; Cosenza et al. 2006; Pozdnyakov et al. 2006; Olorunfemi et al. 2010; Siddiqui and Osman 2013; Gupta et al. 2019).

Among the different geophysical methods, geoelectric methods are one of the cheap and simple geophysical methods available to be employed in solving broad range of engineering problems (Olorunfemi and Meshida 1987; Barker 1997; Adepelumi and Olorunfemi 2000; Olorunfemi et al. 2004; Soupios et al. 2007; Omoloyole et al. 2008; Adepelumi et al. 2009; Adeoti et al. 2009; Fatoba et al. 2010; Ayolabi et al. 2010; Fatoba et al. 2013; Bharti et al. 2016a, b, 2019; Das et al. 2017; Singh et al. 2019; Sivastava et al. 2020; Hamad et al. 2021) especially the applications of geotechnical field investigations (Akintorinwa and Adesoji, 2009; Adeyemo and Omosuyi 2012; Salami et al. 2012; Gupta et al. 2019; Ihtisham et al. 2020).

✉ Wael Dosoky
wael.desoky@sci.svu.edu.eg

1 Faculty of Science, Geology Department, South Valley University, Qena, Egypt

2 Aswan Earthquake Research Center, Aswan, Egypt

At this point, the present study motivates more on mapping the lateral and vertical extent of the different lithological units particularly the expected clayey layer and determines bedrock depth using vertical electrical sounding survey at the new Luxor city. Along with electrical survey, the potential swelling of the foundation beds can be expected by a mineralogical investigation of the clay-rich beds. This work gives the decision-maker and the civil engineers a quick picture about subsurface soil conditions before starting construction of new buildings to manifest the extent to which the subsurface foundation soil of the new Luxor city will be suitable for the constructional purposes in future.

Geology and location of the study area

The new Luxor city is located at the eastern bank of the Nile Valley, 7.5 km southeast of the old Luxor city and 14 km south of the New Tiba city. It covers a surface area of about 18 km^2 (Fig. 1a).

Geologically, the exposed rock units in Luxor area (Fig. 1b) are mainly of sedimentary origin belonging to Upper Cretaceous, Tertiary, and Quaternary deposits. Stratigraphically, the Upper Cretaceous–Early Eocene rock units are unconformably overlain by the Pliocene–Holocene units (Said 1962, 1981 and 1990; Wendorf and Schild 2002; Kamel 2004; El Hossary 1994; Abd El-Rahman 1980).
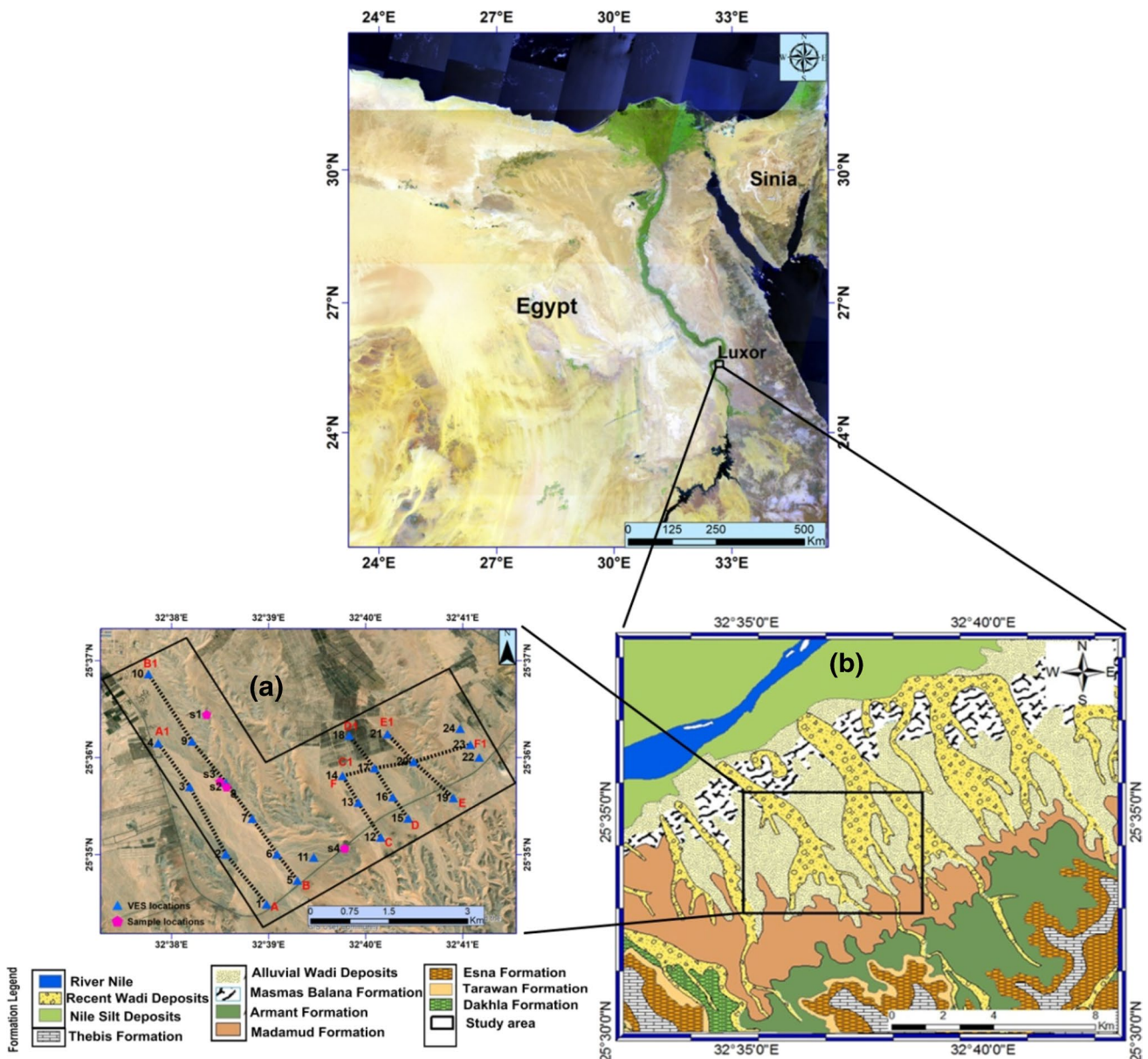

Fig. 1 (a) Location map of Luxorstudy area shows the spatial distribution of VES station and the collected sample (b) Geologic map of Luxor area showing the variousgeologic units included within the study area (modified after Ministry of industry and Mineral Resources previously EGSMA 2006)

Fig. 2 Field view of the studied sections (**a-d**) showing the varied lithology of Madamud Formation and the overlying Quaternary deposits (look at the dashed lines)
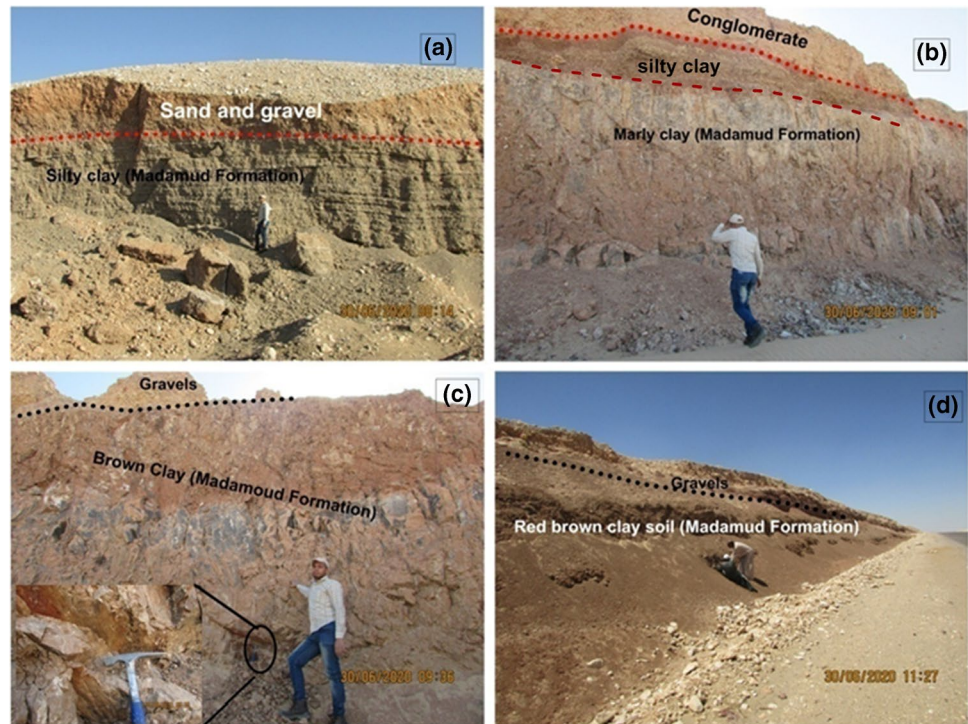
In the Luxor study area, the near-surface Pliocene–Holocene sediments are described as follows: Madamoud Formation (Pliocene unit), Armant and Masmas Ballana Formations (Pleistocene unit), and alluvial wadi deposits (Holocene unit) (Said 1981; Kamel 2004).

The Madamoud Formation is the main geologic formation that outcropped in the study area; it is characterized by red brown clay, marl, and fine-grained sand and silt lamina (Fig. 2).

In addition to the low-grade building materials, the insufficient information about the potentially dangerous subsurface soil conditions such as cavities, faults, cracks, and the presence of clay can lead to collapse of the newly formed constructions. These hazardous sources must be detected before the erection of buildings.

The most predominant sediment types in the investigated area include gravel, conglomerate, clay, silt, marl, and sand (El Hossary 1994; Kamel 2004). Accordingly, the subsurface stratigraphic successions at the studied area are expected to contain clay-rich layers, which can cause detrimental damages to the engineered foundations and buildings due to the swelling-shrinkage behaviour of clay minerals. So, the subsurface lithological characterization of any proposed building site can be performed using an integration between the geoelectrical survey and the mineralogical analysis of the underlying rock units, if the latter are dominated by clay minerals.

Methodology

The objective of vertical electrical sounding technique is to give a detailed information for vertical sequence to different conduction zones in terms of resistivity and thickness below a given point on the ground surface. Considering the purpose of our study for the geological conditions, cost, and operational suitability, vertical sounding was deemed to be appropriate survey method to obtain quick and generalized information about the subsurface layers over a relatively large scale area such as the studied area.

At the present study, twenty-four (VES) data were acquired in the investigated area using ABEM Terrameter SAS 300C resistivity system in a semi-regular grid (Fig. 1a). The spacing interval between stations ranges from 0.5 to 1.4 km depending on the local conditions in the field. Schlumberger configuration was used for vertical electrical sounding data collection where maximum (AB/2) varies from 180 to 250 m according to the accessibility of the measurement site in the field. On the other hand, the potential electrode separation starts at 0.5 m and extends to 40 m. Each VES station is comprised of 31 points of apparent resistivity measurement.

For each VES, the measured apparent resistivity values are plotted against the AB/2 distance on a bilogarithmic paper to correct the deviated measurements and then inverted and interpreted to detect different geoelectric zones

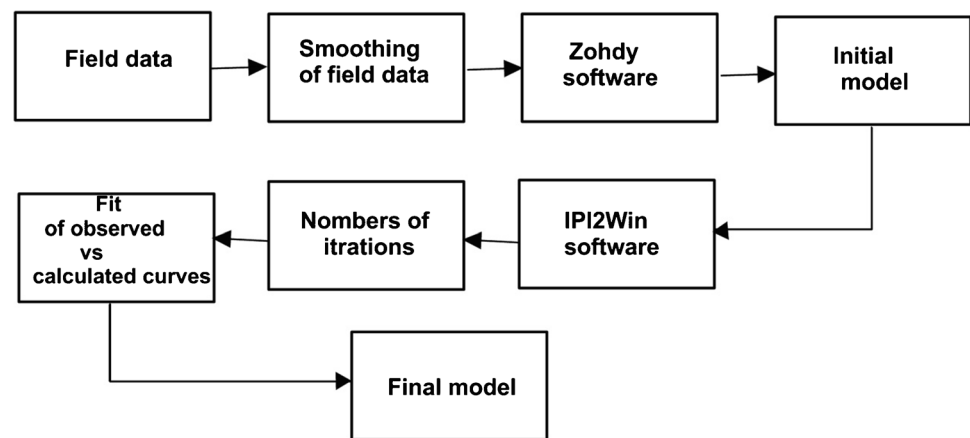**Fig. 3** A typical flow chart of inversion schemes illustrates the interpretation steps

Table 1 Coordinates of the collected samples and its physical description

Sample code	Lat	Long	Physical properties
S1	25.60741	32.63937	Grey and friable
S2	25.59521	32.64250	Dark brown and moderate in hardness
S3	25.59569	32.64204	Red brown and hard
S4	25.58438	32.66308	Brown in colour and friable

in the study area. In order to estimate the true resistivity and thickness values of each unit, two automated inversion software were used: Zohdy's algorithm (Zohdy and Bisdorf 1989) and the IPI2WIN program (Bobatchev et al. 2001). The results obtained from Zohdy and Bisdorf (1989) program and the available geological information were used as a starting model to be further interpreted by the automated inversion IPI2Win software developed by Bobatchev et al. (2001). More numbers of iterations were performed to reach the best fit between the observed and the calculated curves. Figure 3 illustrates a typical flow chart of inversion schemes used in the present study. The interpreted results including layer thicknesses and resistivities were then used to construct a number of geoelectric resistivity cross-sections and subsurface resistivity and thickness maps. These sections and maps were analysed to characterize the subsurface geologic units in the shallow depth less than 50 m in the study area in terms of engineering site characterization.

The bulk mineral composition was studied for 4 samples collected from the clay-rich layers (Madamoud F) of the subsurface lithological successions at four different locations (Fig. 1a). The coordinates and the physical description of these samples are illustrated in Table 1. About 50 g representative powder sample was analysed by X-ray diffractometer, using cu-kα radiation. The XRD machine was set at 4–60 $2\Theta^{\circ}$ angle scanning, 0.06 step size, and a scan rate of 0.06 $2\Theta^{\circ}$/min.

The clay fractions (< 2 µm fraction) were extracted from the four representative clay-rich samples (S1, S2, S3, and S4), which ultrasonically disintegrated using ultrasonic water bath. The samples were treated using 15% H_2O_2 (hydrogen peroxide) for several days to remove all organic materials. The treated samples were then washed on 45-µm sieve using distilled water. The passed fraction was mixed with magnesium chloride solution (0.5 M) to bind the clay particles to each other, and then the clay suspension was pipetted on glass slides of dimension of 2×2.5 cm to form an oriented clay fraction. The later was subjected to three different treatment procedures: untreated (air-dried), treated with ethylene glycol (glycolation at 60 °C for 24 h), and heated at 550 °C for 1 h. These procedures were followed according to El-Habaak et al. (2018). Each type of these treatments was scanned using X-ray diffractometer adjusted at 4–40 $2\Theta^{\circ}$ and step size 0.06. The obtained data were interpreted using X'Pert High Score software.

Results and discussion

Vertical electrical sounding technique

The data obtained from the vertical electrical sounding survey were interpreted qualitatively and quantitatively. The qualitative interpretation of resistivity data was applied to illustrate the general lateral and vertical variations of the apparent resistivity along the selected profiles and to have approximation of the number of geoelectric layers and their aerial distribution in the area under investigation.

All the obtained VES curves are of the QH-type (Fig. 4). This curve type indicates the presence of four geoelectric layers which represent the shallow succession in the study area. The respective resistivity (ρ) of geoelectric layers continuously decrease with depth from the first layer to the third layer and then followed by an increase in the resistivity of

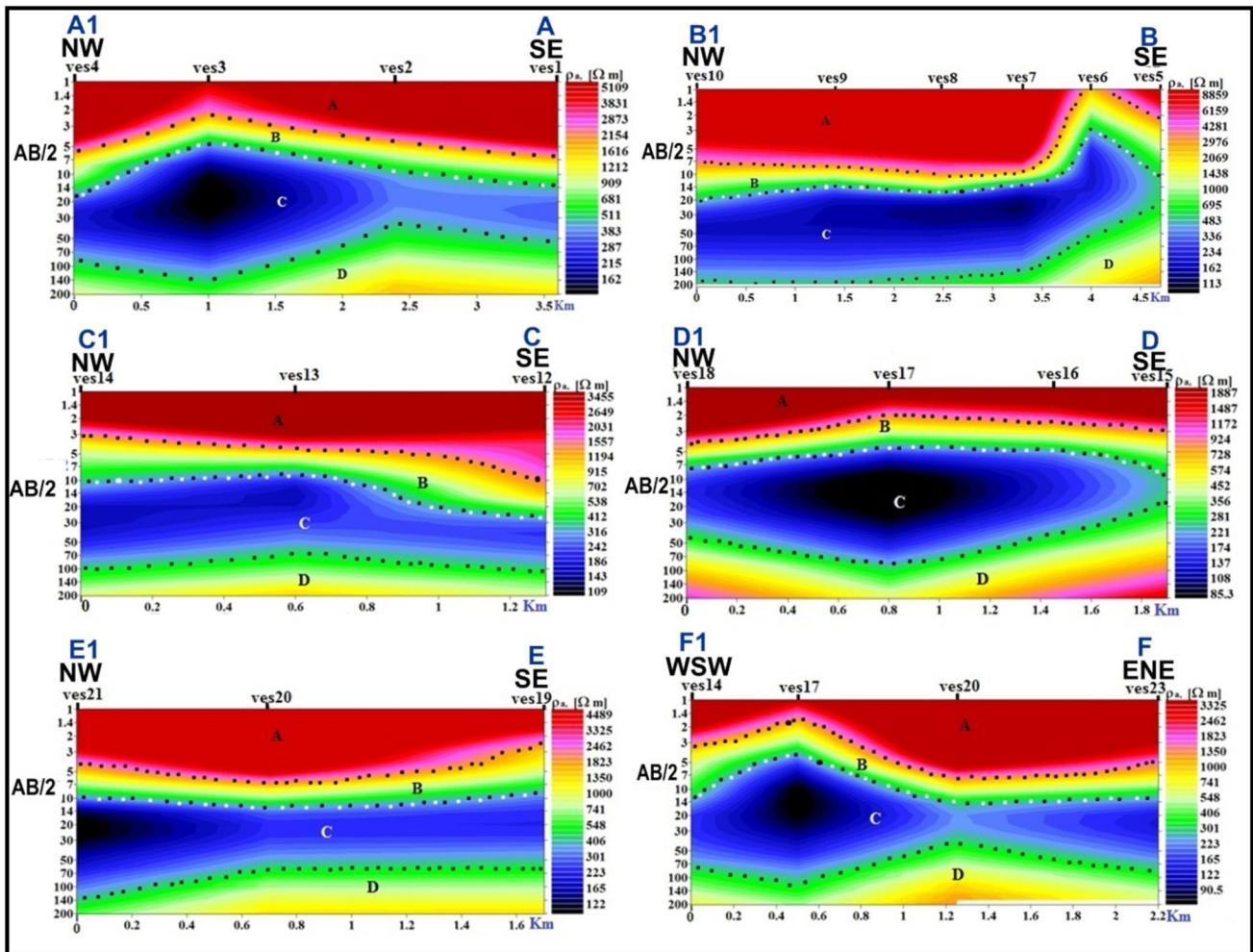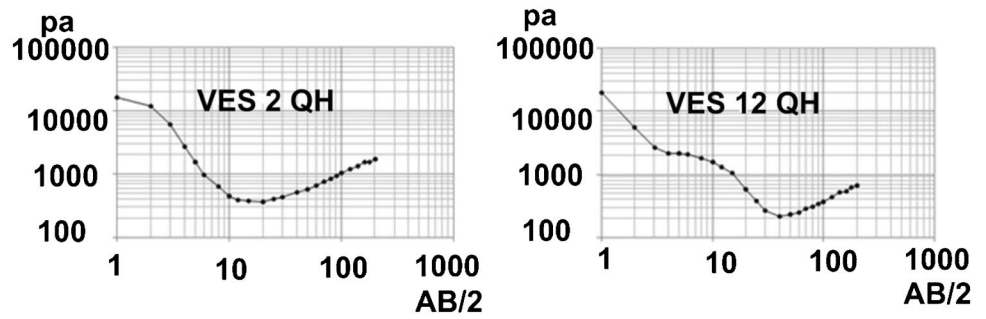**Fig. 4** Example of the VES curves in new Luxor city area

Fig. 5 Pseudo-geoelectriccross-sections along the selected profiles at the study area

the fourth layer. Thus, the resistivities of QH curve can be described as $\rho_1 > \rho_2 > \rho_3 < \rho_4$ where ρ_1 is the resistivity of the upper unit and ρ_4 is the resistivity of the last one. On the other hand, six apparent resistivity pseudo-sections were plotted as colour maps (Fig. 5) to provide approximate picture about resistivity distribution along the selected profiles. Inspection of these sections reflects that the distribution of apparent resistivity in the study area can generally be represented by four different apparent resistivity zones: zone

A (high resistivity), zone B (moderate resistivity), zone C (low resistivity), and zone D (high resistivity). Generally, the apparent resistivity behaviour is the same along all sections, and its distribution might reveal that the subsurface layers are relatively homogeneous in their electric properties at most parts along the selected sections.

Results obtained from the interpretation programs are a number of interpreted geoelectric layers with their corresponding resistivities and thickness. The final results for

Table 2 Results of the interpretation of the measured VES curves

VES No	Lat	Long	ρ_1 (Ω.m)	h_1 (m)	ρ_2 (Ω.m)	h_2 (m)	ρ_3 (Ω.m)	h_3 (m)	ρ_4 (Ω.m)	Depth (m)
1	25.57481	32.64964	25,011	1.58	1058	4.23	255	28.8	7436	34.6
2	25.58342	32.64264	18,868	1.19	851	2.72	305	21.9	3837	25.8
3	25.59567	32.63739	6544	0.85	592	2.06	97.5	25.5	6040	28.4
4	25.60306	32.63175	22,616	1.44	1030	6.78	89.4	14.3	5136	22.5
5	25.57878	32.65458	24,039	0.56	2069	1.82	476	20.7	7193	23.1
6	25.58342	32.65117	4453	0.5	706	1.15	163	14.1	6125	15.8
7	25.58981	32.64769	50,231	2.3	1074	1.39	99.8	25.4	7292	29.1
8	25.59553	32.64247	27,595	2.5	7355	0.748	113	33.5	6444	36.7
9	25.60262	32.63654	19,540	2.5	782	3.61	129	25	2224	31
10	25.61386	32.62842	15,466	2.26	1589	3.6	123	23.8	2871	29.5
11	25.58289	32.65775	24,339	1.62	2018	4.3	165	29.3	3306	35.2
12	25.58667	32.67022	33,848	0.5	2072	7.05	130	29.9	2748	37.5
13	25.59228	32.66533	31,709	0.85	1512	2.05	138	20.8	3189	23.7
14	25.59703	32.66272	22,724	0.643	736	4.18	127	31.9	6369	36.8
15	25.58971	32.67385	23,007	0.5	1095	1.43	227	21.2	6469	23.1
16	25.59328	32.67128	8345	0.5	867	1.26	123	18.4	3905	20.2
17	25.59833	32.66814	6576	0.5	527	1.71	53.5	18.3	2410	20.5
18	25.60372	32.66328	20,955	0.76	1010	1.84	125	18.3	8531	20.9
19	25.59325	32.68169	28,559	0.5	1378	2.61	179	20.9	5439	24
20	25.59947	32.67494	28,456	1.53	1759	3.04	171	22	10,042	26.5
21	25.60428	32.67017	15,670	0.93	1743	2.86	71.3	21.4	4575	25.2
22	25.60011	32.68608	10,129	1.27	442	3.76	181	15.3	5245	20.3
23	25.60183	32.68369	12,081	0.83	2169	2.82	115	30.1	5065	33.8
24	25.60503	32.68289	10,323	0.96	811	3.5	200	20.8	2152	33.3

all inverted sounding curves were summarized in Table 2. Based on the results obtained from the interpretation of sounding curves, six geoelectric cross-sections were constructed with various lengths ranging between 1200 and 4700 m along the chosen profiles that are nearly oriented in NW–SE direction (Fig. 1a). The aim of the executed sections is the investigation and characterization of shallow subsurface strata. These sections are depicted in Fig. 6. Careful inspection of these geoelectric cross-sections reveals that the subsurface succession of the area under investigation comprises four geoelectric layers. The first geoelectric layer is characterized by a high resistivity values ranging between 4453 and 50,231 Ωm due to the high dryness of this layer. It has a thin thickness ranging from 0.5 to 2.5 m. This layer is attributed to the surface layer of dry eroded sand, gravels, and rock fragment intercalated with silt and clay; in addition, and based on field observation, this layer sometimes is composed of compacted conglomerate. The second geoelectric layer is characterized by relatively intermediate resistivity values ranging between 442 and 7355 Ωm. The thickness of this layer varies from 1.15 to 7 m. This layer is supposed to be composed of dry sand and gravels. The third layer is characterized by a relatively low resistivity value with a significant lateral change observed along most of the constructed geoelectric cross-sections. The resistivity values

of this layer range from 53.5 to 476 Ωm with a thickness which varies between 14 and 33.5 m. It is adequate to give a description of this layer in terms of three geoelectric units. The first one has resistivity value which ranges between 163 and 471 Ωm, and it expected to be composed of sandy clay and can be observed at VESes 1 and 2 of profile A-A1 (Fig. 6a), VESes 5 and 6 of profile B-B1 (Fig. 6b), and VES 15 of profile D-D1 (Fig. 6d), existing at the southeastern part of each profile. The second unit has a resistivity values range between 171 and 179 Ωm; this unit is supposed to be a clayey sand which is reported at VESes 19 and 20 (Fig. 6e). It is observed that the resistivity values decrease toward the northwestern direction along each profile forming the third unit with a resistivity value ranges between 53.5 and 138 Ωm which is supposed to be composed of silty clay and marly clay. The last geoelectric layer that is observed along all profiles is characterized by a high resistivity values range between 2152 and 10,042 Ωm. This layer is interpreted as a compacted dry sandstone. The upper surface of this layer lies at depth which varies between 16 and 36.5 m.

The thickness and resistivity of the four geoelectric layers imaged in the constructed cross-sections were mapped; however, only the resistivity, thickness, and depth of the third layer are discussed herein. The contour map (Fig. 7a) shows the resistivity variation of this layer in the study area.
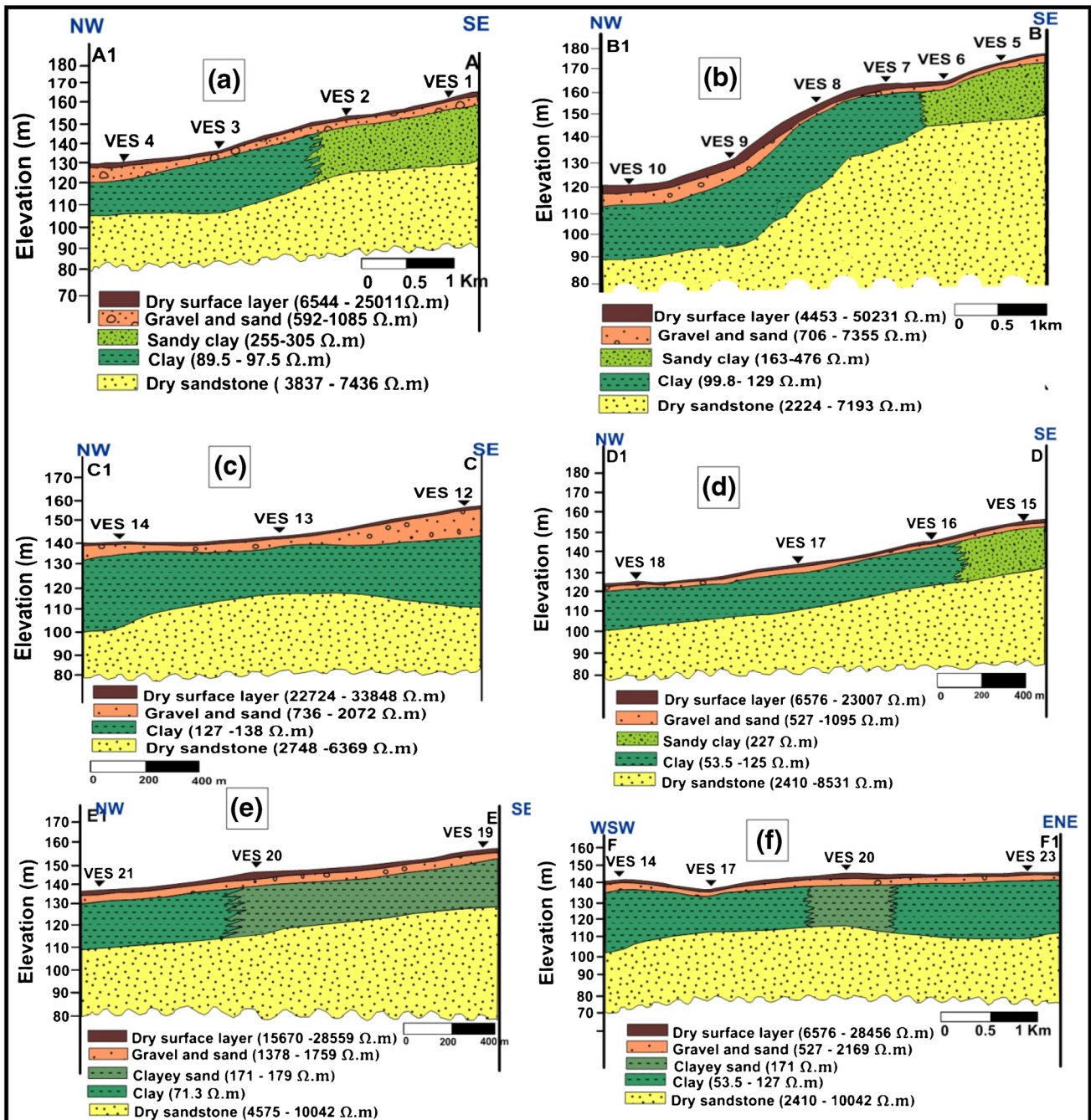
Fig. 6 Geoelectric cross-sectionsalong the selected profiles at the study area

This layer is characterized by a lateral variation of resistivity value since a remarkable decrease of resistivity value is observed toward the northwestern direction, and this may be attributed to the increase of clay content at that direction. Based on the field observations of the exposures and outcrops in the study area (Fig. 2) as well as resistivity values, this layer may be corresponding to the claystone layer that represents the Madamud Formation of the Pliocene age composed mainly of silty clay, marly clay, clayey sand,

and sandy clay. This layer is characterized by lateral facies change, which stands as the main reason behind lateral variation of resistivity values of this layer. The variable thickness distribution of this layer at the study area was manifested in the contour map (Fig. 7b). The upper surface of the third layer lies at a shallow depth ranging between 1.6 and 7.5 m below the surface (Fig. 7c). On the other hand, the maximum depth is observed at the northwestern and the southeastern
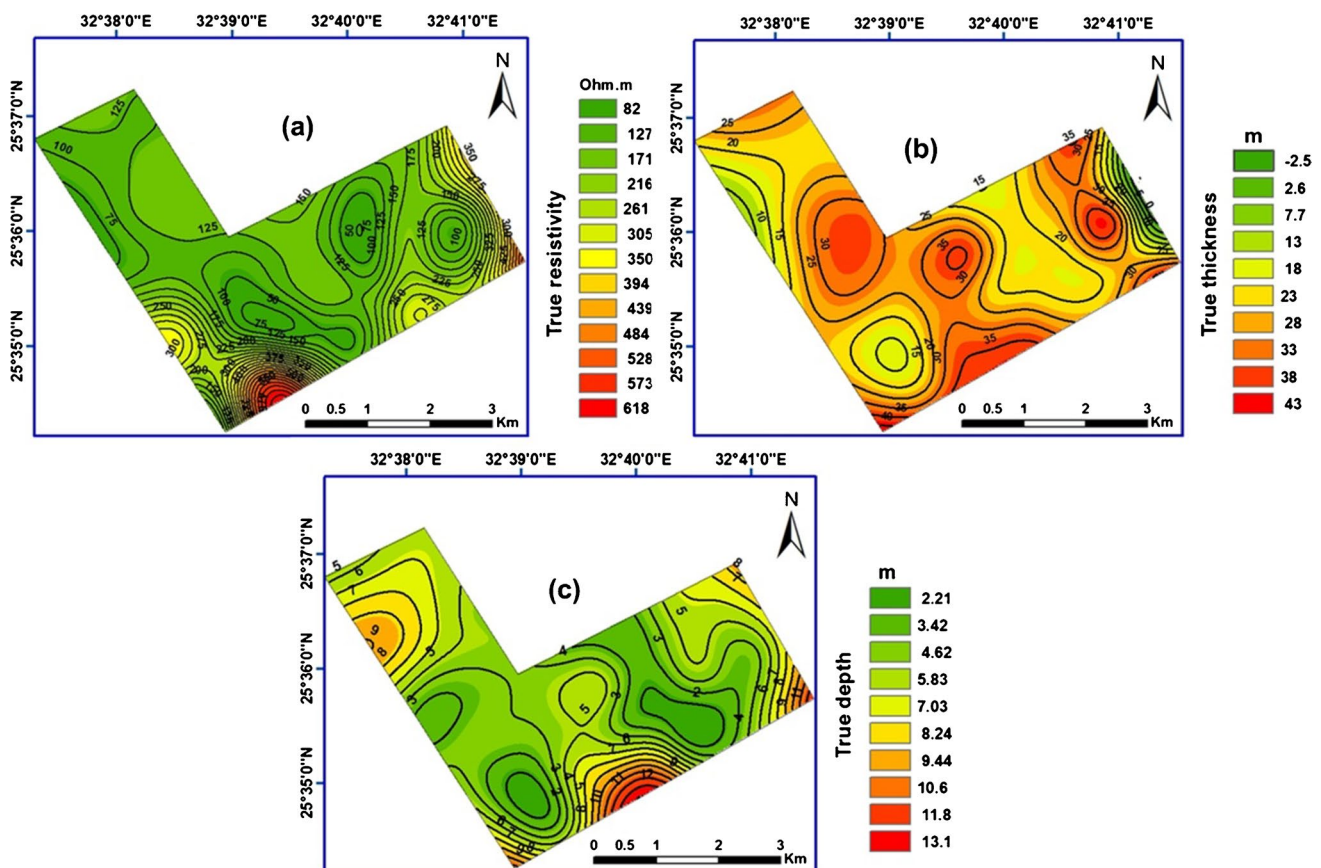
Fig. 7 **a** An isoresistivity, **b** isopach, and **c** depth maps of the claystone layer in the study area

parts of the area, while the rest is characterized by uniform depth.

Bulk mineralogy

XRD patterns of the investigated samples (Fig. 8) reveal the occurrence of non-clay minerals represented by quartz, anhydrite, and calcite. Quartz and calcite are the dominate phases in sample S3, imparting more consolidation compared to the other samples. The clay minerals are detected here as smectite and sepiolite. The occurrence of other clay mineral types is probable, but it cannot be accurately detected by the bulk reflection peaks, as illustrated by S3. So, oriented clay fraction samples were prepared as aforementioned to show whether other clay minerals occur or not.

Clay mineralogy

The interpretation of XRD patterns (Fig. 9) reveals that the < 2 µm clay fraction of the studied clay-rich samples is composed of smectite, kaolinite, chlorite, and illite. Smectite is detected in the air-dried fractions of S1, S2, and S4 at basal reflection of 15.1 Å, which migrated on glycolation

between 18.3 and 19.13 Å and collapsed to 9.8 Å on heating. There is no any noticeable reflection in the glycolated fractions between 5.3 and 8.72 Θ°, indicating the absence of illite–smectite mixed layer (Środoń 1980). The basal reflection of kaolinite appears in S1–S3 at *d* value 7.14 Å without considerable changes on glycolation and heating. Chlorite is only reported in S4 and differentiated from kaolinite by the persistent occurrence of its basal peak on heating at 7.1 Å. Illite is the dominant clay mineral in S3 with similar *d* values of its basal reflection at 10.4 Å, 10.5 Å, and 10.2 Å on air-drying, glycolation, and heating, respectively. It is worth to mention that sepiolite is only observed in the bulk mineralogy and not observed in the XRD patterns of clay fractions due to its fibrous nature (El-Habaak et al. 2020).

Based on the above mention, it is clearly that smectite is the predominate clay mineral of the studied samples. The swelling potentiality of smectite is larger than kaolinite and illite Bergaya et al. (2006). The determination of clay minerals in soils reflects their geotechnical behaviour such as expansive potential Lin and Cerato (2012).

The XRD analysis reflects the abundance of clay minerals in the third units; thus, the main reason behind lowers of the bulk resistivity of soils as it is perspicuous
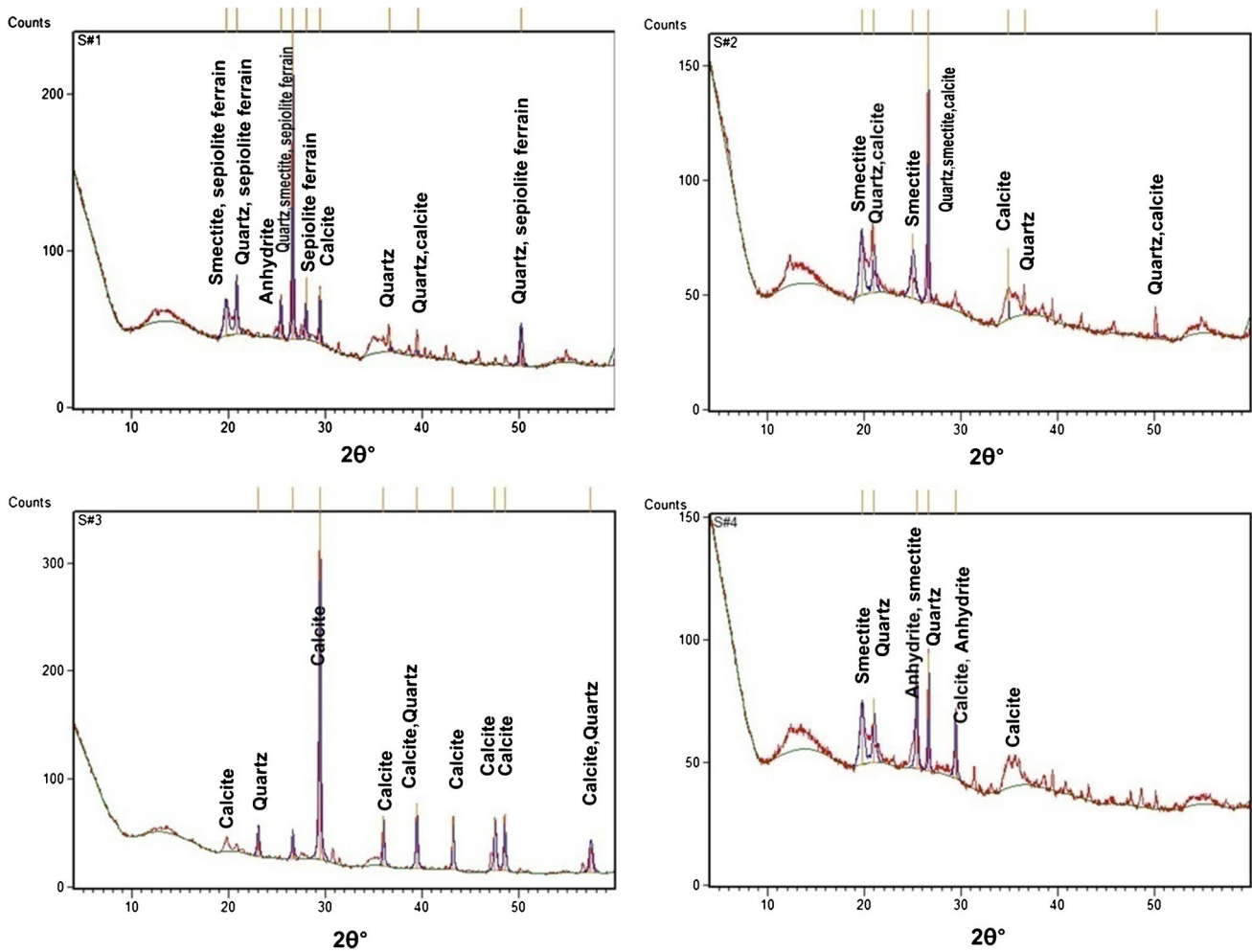
Fig. 8 XRD patterns of samples for bulk mineralogy

from the geoelectric results. Moreover, clay particles may form clay coatings over grains of fine sediments such as silt as a result of repeated wetting and drying. This clay coating can enhance the surface conduction and, consequently, increase the interface conductivity, which results in a decrease of the bulk resistivity of the layer (Mitchell 1993). The XRD analysis reinforces the results obtained from geoelectric resistivity interpretation.

The results obtained from the geoelectric survey alongside mineralogical investigation revealed that clayey layer is distributed laterally along the most part of the study area and extended vertically to a depth reaching to 36.5 m, and this layer is characterized by the presence of expansive minerals. This study highlights the outline of the clayey zone by geoelectric method with its mineralogical composition studies that give a comprehensive knowledge about their geotechnical behaviour and help the engineering structures for choice adequate design for foundation prior construction.

Conclusions

In the present study, geoelectric survey and mineralogical analyses have been used for foundation soil characterization at the proposed site of new Luxor city, Upper Egypt, with the aim of outlining the probable clayey zone presence and to examine the swelling potentiality of this layer.

The subsurface lithological succession at the proposed new Luxor city site is supposed to be characterized by four main geoelectric units, which were interpreted as conglomerate, gravel, and sand intercalated with silt at the top, underlying by sand and gravel unit, beneath it a clay-rich unit mainly silty clay, marly clay, clayey sand, and sandy clay, with dry sand beneath the clayey-rich unit.

The proposed site of new Luxor city is characterized by the presence of the clayey-rich layer which lies at shallow depth that varies between 1.6 and 7 m and its thickness between 14.3 and 33.5 m below the surface. This layer contains expansive clay minerals, mainly smectite as interpreted
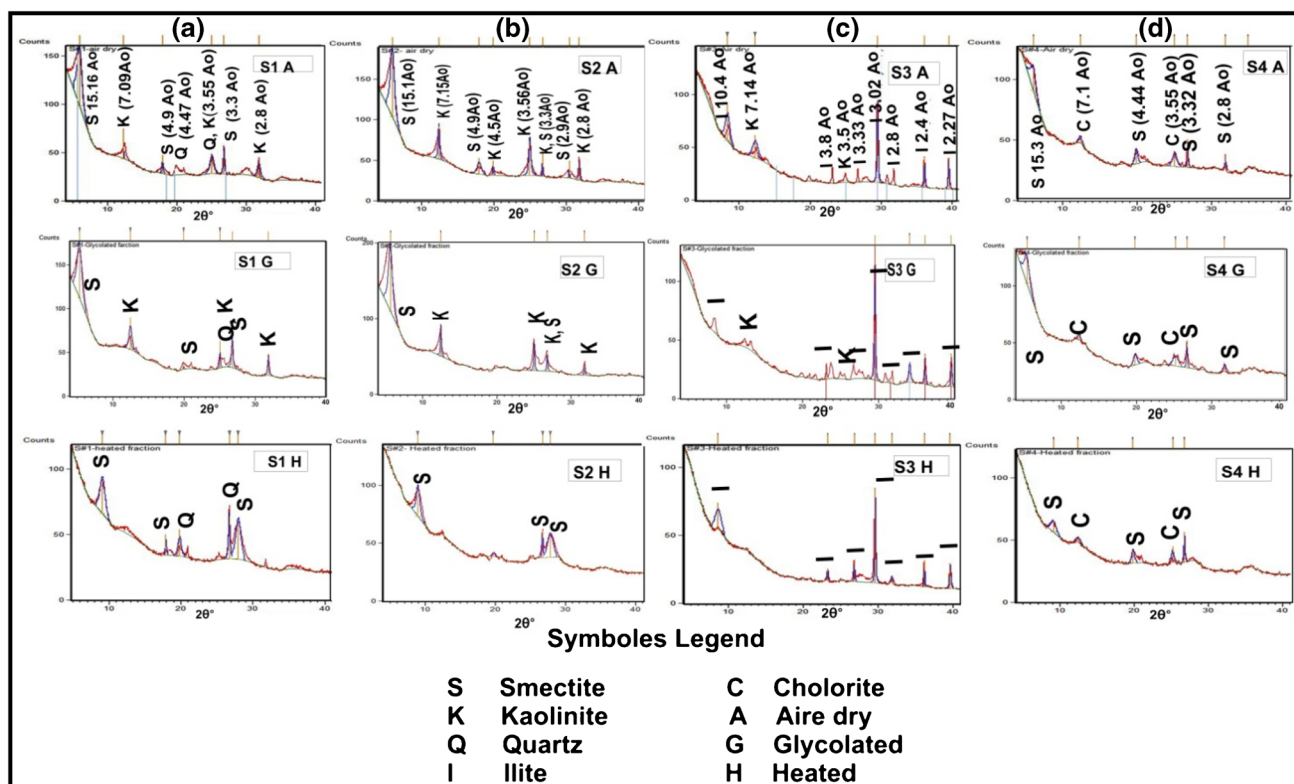
Fig. 9 XRD patterns of < 2μmfraction of **a**) S1, **b**) S2, **c**) S3 and **d**) S4 samples

from the X-ray diffraction analysis. Soils containing smectite clay minerals change in volume (swelling/shrinking) due to moisture content variations. Such variation in clay mineral volume can have a hazardous impact on engineering structures (Fouzan and Muawia 2013).

Recent and present damage, such as subsidence of terrain and cracks in buildings, call for attention to take into consideration the hazardous effect of the delineated clayey layer that can be generated in case of water leakage, which may come from surface irrigation and/or defect in sanitary systems. We recommended improvement of the expansive soil by stabilization or using deeper pile-type foundation to face swelling potential of soil. For safety construction, boreholes are recommended to be drilled at the areas where the clay layer is located at shallow depths to determine the nature of clay minerals present. A more detailed study of the area needs further geotechnical investigation and geophysical studies like seismic refraction method to determine the geotechnical characteristics of the clayey layer.

The present work shows that integration between geo-electric investigation and mineralogical analyses can be used for optimal soil characterization at any construction site of similar condition. The decision-maker should take into account this clay layer for choice of appropriate foundation type during the design and construction stage of building at the proposed site of new Luxor city.

Declarations

Conflict of interest The authors declare no competing interests.

References

Abd El-Rahman MA (1980) Geology of the area southeast of Qena with special reference to the phosphate deposits. Dissertation. Assuit University, Egypt, p 184

Adeoti L, Kehinde I, Adegbola RB, Sovi ST (2009) Foundation investigation using electrical resistivity method: a case study of Iponri, Lagos State, Nigeria. J Eng Res 14(1):50–57

Adepelumi AA, Olorunfemi MO (2000) Engineering geological and geophysical investigation of the reclaimed Lekki Peninsula, Lagos. South West Nigeria Bull Eng Geol Environ 58:125–132

Adepelumi AA, Olorunfemi MO, Faletiba DE, Bayowa OG (2009) Structural mapping of coastal plain sands using engineering geophysical technique: Lagos Nigeria case study. Nat Sci 1:2–9

Adeyemo IA, Omosuyi OG (2012) Hydrogeologic, electrical and electromagnetic measurements for geotechnical characterization of foundation beds at Afunbiowo, near Akure, Southwestern Nigeria. Ind J Sci Tech 5(2):0974–6846

Akintorinwa OJ, Adesoji JI (2009) Application of geophysical and geotechnical investigations in engineering site evaluation. Int J Phys Sci 4(8):443–454

Ayolabi EA, Folorunso AF, Oloruntola MO (2010) Constraining causes of structural failure using electrical resistivity tomography (ERT): a case study of Lagos, Southwestern, Nigeria. J Geophys Min Wealth 156(210):7–18

Barker RD (1997) Electrical imaging and its application in engineering investigations. Engineering Geology Special Publication, Geology Society, London, 12, (1):37–43

Bergaya F, Theng BKG, Lagaly G (2006) Handbook of clay science. Elsevier, Amsterdam

Bharti AK, Pal SK, Priyam P, Kumar S, Srivastava S, Yadav PK (2016a) Subsurface cavity detection over Patherdih colliery, Jharia Coal-Beld, India using electrical resistivity tomography. Environ Earth Sci 75(5):1–17. https://doi.org/10.1007/s12665-015-5025-z

Bharti AK, Pal SK, Priyam P, Pathak VK, Kumar R, Ranjan SK (2016b) Detection of illegal mine voids using electrical resistivity tomography: the case-study of Raniganj coalfield (India). Eng Geol 213:120–132

Bharti AK, Pal SK, Saurabh SKKK, Singh PK, Prakash A, Tiwary RK (2019) Groundwater prospecting by inversion of cumulative data of Wenner-Schlumberger and dipole–dipole arrays: a case study at Turamdih, Jharkhand, India. J Earth Syst Sci 128(4):107. https://doi.org/10.1007/s12040-019-1137-2

Bobatchev A, Modin I and Shevnin V (2001) IPI2WIN Resistivity Sounding Interpretation program, Moscow State University. Moscow, Russia Version 2.0, User's manual p15

Cosenza P, Marmet E, Rejiba F, Cui YJ, Tabbagh A, Charlery Y (2006) Correlation between geotechnical and electrical data, a case study in Garchy in France. J Appl Geophys 60:165–178

Das P, Pal SK, Mohanty PR, Bharti AK, Kumar R (2017) Abandoned mine galleries detection using electrical resistivity tomography method over Jharia coal field, India. J Geol Soc India V90(2):169–174

El Hossary M (1994) Hydrogeological and hydrochemical studies on Luxor area, southern Egypt. MSc Thesis, Ain Shams University, Egypt

El-Habaak G, Askalany M, Abdel-Hakeem M (2018) The effect of mineralogy of calcined shales on the alkali activation and geopolymerization reactions: A case study from Abu-Tartur plateau, Western Desert, Egypt. J Applied clay sci (162):90–100. https://doi.org/10.1016/j.clay.2018.05.025

El-Habaak G, Khalaphallah R, Hassan M, Askalany M, Abdel-Hakeem M (2020) Characterization and exploitation of black shale as unconventional sources of biohydrogen: a case study from Abu-Tartur mine, western Desert, Egypt. Arab J Geosci 13(467):1–15

Fatoba JO, Alo JO, Fakeye AA (2010) Geoelectric imaging for foundation failure investigation at Olabisi Onabanjo University Minicampus, Ago-Iwoye, Southwestern Nigeria. J Appl Sci Res 6(12):2192–2198

Fatoba JO, Salami BM, Adesida A (2013) Structural failure investigation using electrical resistivity method: a case study of Amafor Ihuokpala, Enugu, Southeastern Nigeria. J Geo Min Res 5(8):208–215

Fouzan A, Muawia AD (2013) The study of cracks and fissures phenomenon in Central Saudi Arabia by applying geotechnical and geophysical techniques. Arab J Geosci 7:1157–1164

Gupta RK, Agrawal M, Pal SK, Kumar R, Srivastava S (2019) Site characterization through combined analysis of seismic and electrical resistivity data at a site of Dhanbad, Jharkhand, India. Environ Earth Sci 78(6):226. https://doi.org/10.1007/s12665-019-8231-2

Hamad HA, Mohammed SF, Sattam AA, Mansour SA, Kamal A (2021) Electrical resistivity and refraction seismic tomography in the detection of near-surface Qadimah Fault in Thuwal-Rabigh area, Saudi Arabia. Arab J Geosci 14:1153. https://doi.org/10.1007/s12517-021-07524-2

Ihtisham I, Waqas A, Mehboob UR, Azmat UO, Allah D (2020) Geophysical and geotechnical characterization of shallow subsurface soil: a case study of University of Peshawar and surrounding areas. Arab J Geosci 13:949. https://doi.org/10.1007/s12517-020-05947-x

Kamel ER (2004) Geology of Luxor area and its relationship to groundwater uprising under the Pharaohs Temples. MSc Thesis, Aswan Faculty of Science, South Valley University, Egypt

Legget RF, Karrow PF (1983) Handbook of geology in civil engineering. McGraw-Hill Book Company, New York, p 12.1-12.22

Lin B, Cerato AB (2012) Prediction of expansive soil swelling based on four micro-scale properties. Bull Eng Geol Environ 71(1):71–78

Ministry of industry and Mineral Resources (2006) Geologic map of Luxor (Al UQSUR) Arab Republic of Egypt scale 1:100 000

Mitchell JK (1993) Fundamentals of soil behaviour. Wiley, New York

Okwueze EE, Mbonu EW, Ezeanyim VI, Okon-Umorem, OE (1989) Geophysical investigation for gravel deposits in Ikono Local Government Area of Akwa Ibom State.Nigerian Journal of Physics 2:99–103

Olorunfemi MO, Akintorinwa OJ, Iginla IB, Bayowa GO (2010) Micro-resistivity measurements, near-surface sequence delineation, and empirical relationships with engineering geotechnical parameters. Pac J Sci Technol 11(1):537–544

Olorunfemi MO, Idornigie AI, Coker AT, Babadiya GE (2004) On the application of the electrical resistivity method in foundation failure investigation—a case study. Glob J Geol Sci 2(1):139–151

Olorunfemi MO, Meshida EA (1987) Engineering geophysics and its application in engineering site investigations (case study from IfeIfe area). Nigerian Eng 22:57–66

Omoloyole NA, Oladapo MI, Adeoye OO (2008) Engineering geophysical study of Adagbakuja Newtown Development, Southwestern Nigeria. Medwell Online J Earth Sci 2(2):55–63

Pozdnyakov AI, Pozdnyakova LA, Karpachevskii LO (2006) Relationship between water tension and electrical resistivity in soils. Eurasian Soil Sci 39:S78–S83

Said R (1962) The geology of Egypt. Elsevier, Amsterdam, New York

Said R (1981) The geological evaluation of the river Nile. Publi., New York. Ink, Springier-Verlage, p 151

Said R (1990) The geology of Egypt, 2nd edn. Elsevier, New York, p 1990

Salami BM, Faletiba DE, Fatoba JO, Ajala MO (2012) Integrated geophysical and geotechnical investigation of a bridge site: a case study of a swamp/creek environment in South East Lagos, Nigeria. IFE J Sci 14(1):75–81

Samouëlian A, Cousine I, Tabbagh A, Braund A, Richard G (2005) Electric resistivity survey in soil science: a review. Soil Tillage Res 83:173–193

Siddiqui FI, Osman SBABS (2013) Simple and multiple regression models for relationship between electrical resistivity and various soil properties for soil characterization. Environ Earth Sci 70(1):259–267

Singh KKK, Bharti AK, Pal SK, Prakash A, Saurabh KR, Singh PK (2019) Delineation of fracture zone for groundwater using combined inversion technique. Environ Earth Sci 78:110. https://doi.org/10.1007/s12665019-8072-z

Soupios PM, Georgakopoulos P, Papadopoulos N, Saltas V, Andreadakis A, Vallainatos F, Sarris A, Makris JP (2007) Use of engineering geophysics to Investigate a site for a building foundation. J Geophy Eng 4:94–103

Środoń J (1980) Precise identification of illite/smectite interstratifications by X-Ray powder diffraction. J Clay and Clay Minerals 28(6):401–411

Sivastava S, Pal SK, Kumar R (2020) A time–lapse study using self-potential and electrical resistivity tomography methods for mapping of old mine working across railway tracks in a part of Raniganj coal field, India. Environ Earth Sci 79:332. https://doi.org/10.1007/S12665-020-09067-3

Wendorf F, Schild R (2002) Implications of incipient social complexity in the Late Neolithic in Egyptian Sahara. In: Friedman R (ed) Egypt and Nubia: Gifts of the Desert. British Museum Press, London, pp. 13–20

Zohdy AAR, Bisdorf RJ (1989) programs for the automatic processing and interpretation of Shlumberger sounding curves in Quick BASIC 4.0.U.S. Geological Survey, Open File Report, 89-137, p64